

Binding Modes and Base Specificity of Tris(phenanthroline)ruthenium(II) Enantiomers with Nucleic Acids: Tuning the Stereoselectivity

Jacqueline K. Barton,* Jonathan M. Goldberg,[†] Challa V. Kumar, and Nicholas J. Turro

Contribution from the Department of Chemistry, Columbia University, New York, New York 10027. Received August 29, 1985

Abstract: Binding of tris(phenanthroline)ruthenium(II), $\text{Ru}(\text{phen})_3^{2+}$, enantiomers to nucleic acids of different base compositions and structure was examined by equilibrium dialysis and photophysical methods. Measurement of enantioselectivity combined with photophysical experiments permits the structural characterization of two noncovalent binding modes of the ruthenium(II) complexes to the DNA helix, one intercalatively bound mode showing a strong chiral preference for $\Delta\text{-Ru}(\text{phen})_3^{2+}$ and the other, a surface-bound mode along the DNA major groove, showing a weak preference for $\Lambda\text{-Ru}(\text{phen})_3^{2+}$. Luminescence decay of $\text{Ru}(\text{phen})_3^{2+}$ isomers in the presence of DNA shows components of two different lifetimes. Quenching of the emission with ferrocyanide results in nonlinear Stern–Volmer plots. Finite polarization in the emission of both Δ - and $\Lambda\text{-Ru}(\text{phen})_3^{2+}$ in the presence of DNA is indicative of intercalation; greater polarization is found consistently for $\Delta\text{-Ru}(\text{phen})_3^{2+}$ with DNA. The total binding affinity of $\text{Ru}(\text{phen})_3^{2+}$ to DNA is ionic strength dependent in a manner consistent with the release of 2.2 counterions per bound ruthenium. Although binding to DNA of $\text{Ru}(\text{phen})_3^{2+}$ shows no clear dependence on the guanine–cytosine (GC) content of the DNA, variations in enantiomeric preferences both as a function of GC content and as a function of ionic strength are observed. Chiral discrimination for $\Delta\text{-Ru}(\text{phen})_3^{2+}$ increases both with the percent GC and with increasing Na^+ concentration. Based upon the stereoselectivities found by steady-state emission polarization, the variations are attributed to changes in chiral preferences for intercalation. This variation may indicate local changes in DNA groove size, e.g. a compression along the helix axis direction with increasing ionic strength or increasing percent GC. Weak surface binding, having a preference for $\Lambda\text{-Ru}(\text{phen})_3^{2+}$, is observed with double-stranded RNA. For both $\text{Ru}(\text{phen})_3^{2+}$ and $\text{Ru}(\text{DIP})_3^{2+}$ (DIP = 4,7-diphenylphenanthroline), binding to T4 DNA glycosylated in the major groove is markedly diminished compared to binding to calf thymus DNA. The chiral ruthenium complexes, with luminescence characteristics indicative of binding modes, and stereoselectivities that may be tuned to the helix topology, may be useful molecular probes in solution for nucleic acid secondary structure.

The design of small molecules that target specific sites along a DNA helix has become a subject of considerable interest.^{1–7} Small molecules serve as analogues in studies of protein–nucleic acid recognition, provide site-specific reagents for molecular biology, and yield rationales for new drug design. Many small molecule based chemical reagents have already been proven to be useful as sensitive probes of local nucleic acid structure.

We have concentrated on a study of the consequences of incorporating stereochemistry (chirality) into small inorganic complexes that bind to nucleic acids. Chiral discrimination has been observed for intercalation of tris(phenanthroline)metal complexes into DNA helices,⁸ in the covalent interactions of bis(phenanthroline)ruthenium(II) with DNA,⁹ and in photoactivated cleavage reactions of cobalt(III) complexes along the helical strand.¹⁰ Electric dichroism studies also have supported the stereoselective binding of ruthenium(II) complexes to B DNA.¹¹ Moreover, this enantiomeric selectivity has been particularly valuable in designing probes to distinguish between the right-handed B DNA and left-handed Z DNA conformations.¹²

The utility of chiral complexes as site-selective nucleic acid structural probes becomes apparent as well in studies with B DNA. We report here a detailed characterization of the interaction of tris(phenanthroline)ruthenium(II) isomers (Figure 1) with double-stranded polynucleotides. By use of both classical and photophysical techniques, interactions of these probes with DNAs of differing guanine–cytosine content, with RNAs, and as a function of ionic strength have been examined. The photophysical methods used here have allowed us to identify and specifically characterize two modes of binding. Sequence-dependent variations in enantioselectivity are observed for the intercalative mode and additionally for an electrostatic association of the chiral ruthenium(II) cations along the helix. These observations point out subtle sequence-specific differences in local structure that may be detected by using these small molecule probes and furthermore provide a rational and systematic basis for the design of new probes

for helical conformations based upon groove associations.

Experimental Procedures

Buffers and Chemicals. All experiments were carried out at pH 7.2 with distilled deionized water in buffers containing 5 mM Tris–HCl. In addition buffers 1–7 contained, respectively, 50, 75, 100, 125, 150, 175, and 200 mM NaCl. $\text{K}_4\text{Fe}(\text{CN})_6$ was Aldrich Gold Label, and CoCl_2 was obtained from Alfa Chemical Co.; both were used without further purification. Spectra-Por-2 dialysis tubing (12 000–14 000 MWCO), obtained from Fisher Scientific, was prepared as described previously.^{8a}

Ruthenium Complexes. Tris(phenanthroline)ruthenium(II) dichloride, $[\text{Ru}(\text{phen})_3]\text{Cl}_2$, and tris(4,7-diphenylphenanthroline)ruthenium(II) dichloride, $[\text{Ru}(\text{DIP})_3]\text{Cl}_2$, were synthesized, and enantiomers were separated as described previously.¹² Resolution of $\text{Ru}(\text{phen})_3^{2+}$ enantiomers gave typically isomeric purities of 93% and 95% for Λ and Δ isomers, respectively. $\Delta\text{-Ru}(\text{DIP})_3\text{Cl}_2$ had an enantiomeric purity of 87%. If the prefix Λ or Δ is not before the metal, *rac* is assumed.

Nucleic Acids. *Clostridium perfringens* DNA, T4 DNA, calf thymus DNA, *Micrococcus lysodeikticus* DNA, and yeast tRNA were obtained

(1) Barton, J. K. *Comments Inorg. Chem.* **1985**, *3*, 321–348.

(2) (a) Schultz, P. G.; Taylor, J. S.; Dervan, P. B. *J. Am. Chem. Soc.* **1982**, *104*, 6861–6863. (b) Hertzberg, R. P.; Dervan, P. B. *J. Am. Chem. Soc.* **1982**, *104*, 313–34.

(3) Berman, H. M.; Young, P. R. *Annu. Rev. Biophys. Bioeng.* **1981**, *10*, 87.

(4) Waring, M. *Annu. Rev. Biochem.* **1981**, *50*, 159–192.

(5) Lippard, S. J. *Science (Washington, D.C.)* **1982**, *218*, 1075.

(6) Dabroviak, J. C. *Life Sci.* **1983**, *32*, 2915–2931.

(7) Hecht, S. M., Ed. *Bleomycin: Chemical, Biochemical and Biological Aspects*; Springer-Verlag: New York, 1979.

(8) (a) Barton, J. K.; Danishefsky, A. T.; Goldberg, J. M. *J. Am. Chem. Soc.* **1984**, *106*, 2172–2176. (b) Barton, J. K.; Dannenberg, J. J.; Raphael, A. L. *J. Am. Chem. Soc.* **1982**, *104*, 4967–4969. (c) Kumar, C. V.; Barton, J. K.; Turro, N. J. *J. Am. Chem. Soc.* **1985**, *107*, 5518–5523.

(9) Barton, J. K.; Lolis, E. *J. Am. Chem. Soc.* **1985**, *107*, 708–709.

(10) Barton, J. K.; Raphael, A. L. *J. Am. Chem. Soc.* **1984**, *106*, 2466–2468.

(11) (a) Yamagishi, A. *J. Chem. Soc., Chem. Commun.* **1983**, 572–573.

(b) Yamagishi, A. *J. Phys. Chem.* **1984**, *88*, 5709–5713.

(12) (a) Barton, J. K.; Basile, L. A.; Danishefsky, A. T.; Alexandrescu, A. *Proc. Natl. Acad. Sci. U.S.A.* **1984**, *81*, 1961–1965. (b) Barton, J. K.; Raphael, A. L. *Proc. Natl. Acad. Sci. U.S.A.* **1985**, *82*, 6460–6464.

[†] Present address: Department of Biochemistry, University of California, Berkeley, CA 94720.

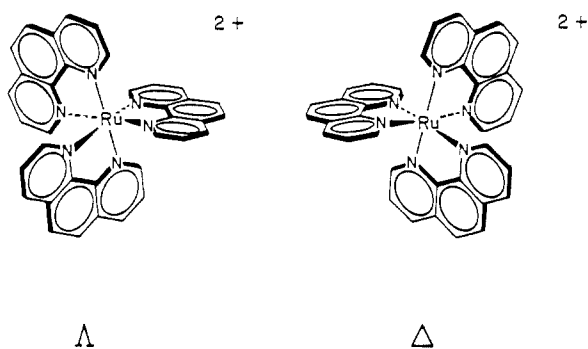


Figure 1. Enantiomers of tris(phenanthroline)ruthenium(II), $\text{Ru}(\text{phen})_3^{2+}$.

from Sigma Chemical Co. and purified by phenol extraction. The synthetic ribo- and deoxyribonucleotide polymers were obtained from P-L Biochemicals. All nucleic acid solutions were extensively dialyzed to bring them to appropriate ionic strengths and to remove small fragments. DNA concentrations were determined spectrophotometrically¹³ by using the following molar extinction coefficients ($\text{M}^{-1} \text{cm}^{-1}$) at 260 nm: *Cl. perfringens*, 6200;¹⁴ T4, 8000;¹⁴ calf thymus, 6600;¹⁴ *M. lysodeikticus*, 6900;¹⁴ yeast tRNA, 7700;¹⁵ poly(dAdT)·poly(dAdT), 6600;¹⁶ poly(dGdC)·poly(dGdC), 8400;¹⁷ poly(A)·poly(U), 7140;¹⁸ poly(I)·poly(C), 5000.¹⁹

Equilibrium Dialysis. One-milliliter of retentates containing 1 mM nucleotide solutions were dialyzed first against buffer and then against 3.25-mL dialysates containing $[\text{Ru}(\text{phen})_3](\text{ClO}_4)_2$ concentrations ranging from 10 to 100 μM for 24 h, after which time equilibration was achieved. The solutions were kept in the dark to avoid photocleavage reactions.²⁰ Temperatures were held at 25 °C, and the samples were shaken at a constant rate. Upon equilibration, dialysates, and retentates were separated and diluted to give absorbances between 0.5 and 1.0 to facilitate spectral analysis. Bound and free concentrations were determined on the basis of absorbance readings at 447 nm²¹ since hypochromic effects were negligible at these dilutions.

Spectroscopic Measurements. All absorption spectra were measured with either a Varian Cary 219 spectrophotometer or a Perkin-Elmer 559A spectrophotometer. Circular dichroic measurements were made with a Jasco J-40 automatic recording spectropolarimeter. All luminescence measurements were conducted by using a Perkin-Elmer LS-5 fluorimeter at 20 °C in appropriate buffer solutions. Samples were excited at 464 nm, and the emission was monitored at 600 nm for all the emission titration experiments. In these experiments, small aliquots (10–12 μL) of concentrated solutions of the nucleic acid (2 mM nucleotide) were added to 4 μM ruthenium solutions in 1-mL volumes. To keep the concentration of ruthenium constant, the nucleic acid stock solutions contained equal concentrations of ruthenium. All solutions were allowed to equilibrate thermally for ~ 15 min before measurements were made. Quenching experiments were conducted by adding 5–20- μL aliquots of a 20 mM ferrocyanide stock solution to 1–2-mL samples containing from 100 to 200 μM nucleic acid concentrations in buffers 1–7. Metal to DNA phosphate ratios were varied from 1:20 to 1:40. Gel electrophoretic analysis of superhelical DNAs after incubation with these conditions showed no effect on nucleic acid tertiary structure. Additionally, results of an equilibrium dialysis experiment were unchanged in the presence of ferrocyanide.

Polarization Studies. Steady-state emission polarization measurements were made on an SLM 4600 spectrophotometer employing Glan-Thompson calcite prism polarizers arranged in a "T"-shaped geometry. Samples were excited at 482 nm, and the emission was monitored by employing Corning 2-73 glass filters. The orientation of the polarizers was checked with glycogen solutions. In addition, polarization of $\text{Ru}(\text{bpy})_3^{2+}$ in glycerol agreed well with reported values.²² All solutions

were equilibrated in a thermostated cell holder at 20 °C for at least 15 min in order to achieve stable readings. Ruthenium concentrations used typically were 2–4 μM . Several readings were averaged for a single measurement, and the deviation was usually less than 5%.

Lifetime Measurements. The luminescence lifetimes were measured with a single photon counting unit using a PRA 1000A lamp and Ortec electronics and a TN-1710 MCA interfaced with an HP 87 personal computer. The decay traces were deconvoluted with software developed by Dr. C. Doubleday, in our laboratory. Appropriate filters were used for both excitation and emission to minimize the scattered light. The lifetime measurements were determined for air-saturated solutions at 20 °C in a thermostated cell holder. The lifetimes were reproducible within $\pm 5\%$.

Stereoselectivity. Measurements of the degree of stereoselectivity in binding ruthenium complexes to the polynucleotides were made and calculated from equilibrium dialysis experiments of racemic mixtures, as described previously.^{8a} The difference in chemical shifts ($\Delta\epsilon$) of H2 protons of the two enantiomers upon addition of the shift reagent (0.732 ppm) was used to determine the purities of the two enantiomers.²³ The parameter *S* is defined here as the ratio of bound Δ isomer to total bound ruthenium complex. To determine *S* in emission polarization experiments using pure isomers, the ratio of ($P_\Delta - P_\Lambda$) to ($P_\Delta + P_\Lambda$) was determined by measuring polarization for each isomer (P_Δ and P_Λ) under the same conditions.

Results

Characterization of Binding Modes. In this paper we propose to consider two primary modes of binding of $\text{Ru}(\text{phen})_3^{2+}$ to nucleic acids: (a) intercalation and (b) surface binding. Intercalative binding allows a close approach of the metal complex to the helix as one of the ligands is sandwiched between the adjacent base pairs. This mode of binding would lead to a substantial perturbation in the photophysical properties of the metal complex such as emission lifetimes and intensities as well as steady-state polarization. In addition, intercalation imposes constraints on rotational degrees of freedom and can enhance the emission polarization. The stereoselectivity associated with this binding mode would be very sensitive to (i) the stereochemistry (chirality) of the metal complex, (ii) matching the symmetry of the metal complex to the helix topography, and (iii) DNA groove size.

In contrast, surface binding provides stabilization due to hydrophobic and electrostatic interactions. The complex would be relatively free to diffuse along the helix surface. The stereochemistry of this mode of binding, however, still could be very sensitive to the topography as well as groove size. Intercalation and surface binding modes will be considered throughout this paper for discussion; however, a third mode of binding, a nonspecific ionic association, may always occur. This last binding mode would be insensitive to the helix handedness or groove size. The following are a series of experiments that characterize and distinguish interactions of $\text{Ru}(\text{phen})_3^{2+}$ cations with nucleic acids in terms of surface binding and intercalation.

Equilibrium Dialysis. Classical dialysis experiments were used to assay total binding of the ruthenium complex to the polynucleotide. The binding affinity of tris(phenanthroline)metal complexes to DNA is low, as reported previously,^{8a} but additionally shows a substantial dependence on ionic strength. Dialysis experiments were conducted at 25 °C in buffers with sodium ion concentrations ranging from 50 to 200 mM. Scatchard plots were obtained for each ionic strength, and the intrinsic binding constant $K(0)$, was determined by extrapolating linear plots to zero values of *r*, the ratio of bound ruthenium to nucleotide. The inverse binding site size (per nucleotide), or *n* value using a Scatchard analysis,²⁴ was constrained to a value of 0.125 for all buffers based upon the earlier nonlinear least-squares analysis of a saturation site size of four base pairs.^{8a}

Figure 2 shows the dependence of $K(0)$ on the ionic strength of the medium, expressed as the total positive ion concentration, $[\text{M}^+]$, in solution. The binding affinity decreases appreciably with increasing ionic strength. The linear relationship for a plot of log

(13) Morrison, W. R. *Anal. Biochem.* **1964**, *7*, 218–224.

(14) Felsenfeld, G.; Hirschman, S. Z. *J. Mol. Biol.* **1965**, *13*, 407.

(15) Tissieres, A. *J. Mol. Biol.* **1959**, *1*, 365–374.

(16) Inman, R. B.; Baldwin, R. L. *J. Mol. Biol.* **1962**, *5*, 172–184.

(17) Wells, R. D.; Larson, J. E.; Grant, R. C.; Shortle, B. E.; Cantor, C. R. *J. Mol. Biol.* **1970**, *54*, 465–497.

(18) Schmechel, D. E. V.; Crothers, D. M. *Biopolymers* **1971**, *10*, 465.

(19) Chamberlin, M. J.; Patterson, D. L. *J. Mol. Biol.* **1965**, *12*, 410.

(20) Danishefsky, A. T., unpublished results in our laboratory.

(21) Lin, C. T.; Bottcher, W.; Chou, M.; Creutz, C.; Sutin, N. *J. Am. Chem. Soc.* **1976**, *98*, 6536.

(22) Fujita, I.; Kobayashi, H. *Inorg. Chem.* **1973**, *12*, 2758.

(23) Barton, J. K.; Nowick, J. S. *J. Chem. Soc., Chem. Commun.* **1984**, 1650–1652.

(24) Scatchard, G. *Ann. N.Y. Acad. Sci.* **1949**, *51*, 660.

Table I. Features in Binding Ru(phen)₃²⁺ Enantiomers to DNAs of Varying Base Sequences

DNA	% GC	K(0) × 10 ⁻³ , M ⁻¹	Stern-Volmer slope × 10 ⁻² , M ⁻¹			emission lifetimes, ns			polarization	
			rac	Δ	Λ	rac	Δ	Λ	Δ	Λ
poly[d(AT)]	0	9.2	3.0	3.8	2.0	412 (426) ^a 1076 (487)			0.0199	0.0196
<i>Cl. perfringens</i>	26	9.8	3.7	5.9	4.2	563 (801) 2211 (184)	502 (705) 1587 (284)	539 (741) 1851 (253)	0.0301	0.0267
calf thymus	42	6.2	4.4	2.5	3.7	505 (700) 1233 (245)	559 2137	583 1999	0.0367	0.0258
<i>M. lysodeikticus</i>	74	10.0	3.7	3.8	7.3	509 (807) 1309 (130)	677 1864		0.0206	0.0094
poly[d(GC)]	100	4.0	5.5				581 (690) 708 (270)	531 (1000)	0.0132	0.0060

^a Values in parentheses correspond to the preexponential weighting factors obtained in solving the decay curves as a biexponential. Although not strictly quantitative, these coefficients reflect the amplitude of short- and long-lived components in the ruthenium-DNA samples.

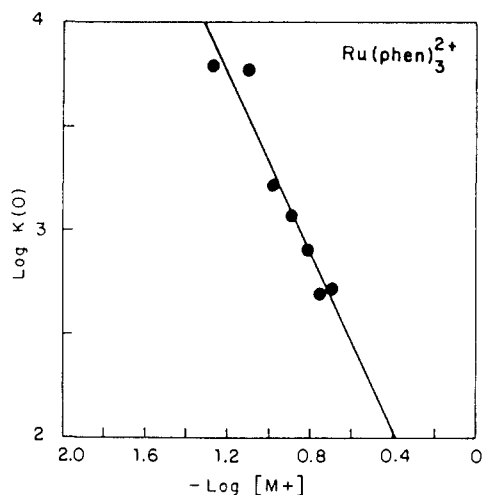


Figure 2. Variations in the intrinsic binding constant, $K(0)$, as a function of ionic strength for rac -Ru(phen)₃²⁺ with calf thymus DNA. The total positive ion concentration, $[M^+]$, is determined as the summation of sodium and Tris cation concentrations in the medium.

$K(0)$ vs. $\log [M^+]$ may be described in terms of the following equation:²⁵

$$\log K(0) = -n\psi \log [M^+] + \delta \log K_{1M} \quad (1)$$

where $n\psi$ expresses the number of monovalent counterions released from the polynucleotide on binding the metal complex to a site containing n' phosphate residues, ψ then corresponds to the extent of counterion binding per phosphate before association with the metal complex, and K_{1M} is the intrinsic binding constant in 1 M sodium ion. The electrostatic component, given by the slope of 2.2, indicates that binding of the ruthenium dication releases 2.2 monovalent counterions from the polymer. Interestingly, this slope is identical with that found in binding the divalent but planar metallointercalator (phen)Pt(en)²⁺ (en = ethylenediamine) to DNA.²⁶ The value of the intrinsic binding constant, however, which includes the intercalative component, is lower for the octahedral Ru(phen)₃²⁺ than that found for (phen)Pt(en)²⁺; at 100 mM NaCl $K_{Ru}(0) = 2130 \text{ M}^{-1}$ while $K_{Pt}(0) = 1.8 \times 10^5 \text{ M}^{-1}$. Thus, binding of Ru(phen)₃²⁺ involves strong electrostatic interactions and causes release of counterions.

Optical enrichment in equilibrium dialysis experiments with racemic mixtures of the metal complexes and nucleic acids provides an excellent measure of stereoselectivity for the overall binding of these metal complexes to nucleic acids (vide infra).

Luminescence Quenching. Luminescence quenching experiments, among other techniques, show clearly the presence of more than one binding mode for Ru(phen)₃²⁺ with nucleic acids. The

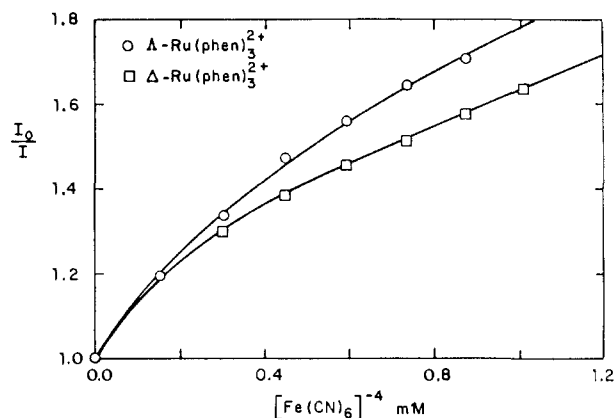


Figure 3. Luminescence quenching of Δ (□) and Λ (○) Ru(phen)₃²⁺ bound to calf thymus DNA (DNA phosphate:Ru = 40) with increasing concentrations of $\text{Fe}(\text{CN})_6^{4-}$. The differing slopes for the isomers reflect the enantioselectivity of binding the ruthenium complexes to the DNA.

luminescence intensities and lifetimes from the ruthenium polypyridine complexes,^{21,27} upon visible excitation, are enhanced on binding to DNA. Quenching of this luminescent excited state with the use of an anionic quencher such as $\text{Fe}(\text{CN})_6^{4-}$ allows the discrimination of different bound ruthenium species.^{8c} Figure 3 shows a Stern-Volmer plot for luminescence quenching of ruthenium-DNA solutions (DNA phosphate to ruthenium ratio of 40) with increasing concentrations of ferrocyanide. The curves do not show simple linear behavior as would be expected for a single-component donor-quencher system. Instead, a downward curvature is found, indicating the differential accessibility of bound ruthenium species to the quencher. Ferrocyanide quenches Ru(phen)₃²⁺ excited state with high rates when free in solution (slope $4.9 \times 10^3 \text{ M}^{-1}$), higher than the rate calculated from either slope shown in Figure 3. Therefore, for these DNA to ruthenium ratios the curvature indicates a mixture of bound (rather than bound plus free) forms. The efficiency of ferrocyanide quenching of ruthenium bound to DNA is decreased relative to the free ruthenium, because the bound ruthenium cations are protected from the anionic water-bound quencher by the array of negative charges along the DNA phosphate backbone. The curvature reflects differing degrees of protection or relative accessibility of bound cations. A small value for late slopes (at $>0.5 \text{ mM}$ ferrous ion concentrations) in these curves represents low accessibility of the bound ruthenium species to the anionic quencher. The slope can therefore be taken as a measure of total binding affinity, a large slope corresponding to poor protection and low binding.

Shown in Figure 3 are the ferrocyanide quenching curves for Δ - and Λ -Ru(phen)₃²⁺ in the presence of calf thymus DNA. At high concentrations, $\sim 0.5 \text{ mM}$ ferrocyanide, the K_{SV} value is 250 M^{-1} for the Δ isomer and 370 M^{-1} for the Λ isomer. The dif-

(25) (a) Manning, G. S. *Q. Rev. Biophys.* **1978**, *11*, 179-246. (b) Record, M. T., Jr.; Anderson, C. F.; Lohman, T. M. *Q. Rev. Biophys.* **1978**, *11*, 103-178.

(26) Howe-Grant, M.; Lippard, S. J. *Biochemistry* **1979**, *18*, 5762.

(27) (a) Hager, G. D.; Crosby, G. A. *J. Am. Chem. Soc.* **1975**, *97*, 7031. (b) Hager, G. D.; Watts, R. J.; Crosby, G. A. *J. Am. Chem. Soc.* **1975**, *97*, 7037. (c) Elfring, W. H., Jr.; Crosby, G. A. *J. Am. Chem.* **1981**, *103*, 2683.

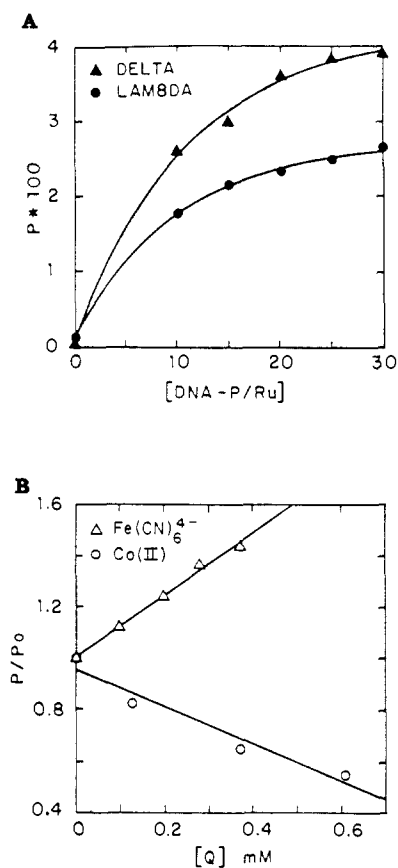


Figure 4. Steady-state polarization, P , in the emission of $Ru(phen)_3^{2+}$ bound to DNA. (A) Increasing concentrations of DNA yield an increase in polarization. The differing polarization for the isomers may reflect enantioselectivity of intercalation. (B) Quenching of the polarized emission is found by a cationic quencher, cobaltous ion (O), which binds to DNA, but P is enhanced in the presence of the anionic quencher $Fe(CN)_6^{4-}$ (Δ).

ferential quenching is consistent with the relative binding of the two isomers to the helix. The curves thus reflect the enantiomeric preference of Δ - $Ru(phen)_3^{2+}$ in binding to calf thymus DNA. Similar curves were observed for other nucleic acids, and the corresponding slopes are included in Table I.

Emission Polarization. The two binding modes, one of which appears to be predominantly surface bound and the other intercalative, may be distinguished by steady-state emission polarization experiments. An intercalatively bound form, held more rigidly in the helix with long residence times on the time scale of the emission lifetimes, should yield finite polarization, while a more flexible surface binding along the groove would not contribute significantly to the polarization. Figure 4A shows the increase in polarization with increasing nucleic acid concentrations, leveling off at a DNA phosphate to ruthenium ratio of $\sim 30:1$, when most of the ruthenium is bound. The maximum polarization observed is substantially less than the limiting value of 0.14 seen for $Ru(bpy)_3^{2+}$ in a matrix,²² but the value could be reduced because of the motions of the double helix, the long luminescent lifetimes, and the finite residence times, all of which would contribute to a decrease in the steady-state polarization. Shown in Figure 4A are the curves for Δ and Λ isomers. Here again it is evident from the greater polarization that the Δ isomer is preferred over the Λ isomer for intercalation into calf thymus DNA. The overall selectivity for the Δ isomer therefore arises primarily due to the intercalative mode of binding into the right-handed B-form calf thymus DNA. This feature will be discussed further.

By appropriately choosing ionic quenchers, it is possible to selectively quench either the bound or the free ruthenium excited states. For example, ferrocyanide was employed above to quench the emission from the free form at a much faster rate than that of any bound form. These quenching experiments were coupled

with polarization measurements to show that the steady-state polarization is indeed due to the bound ruthenium complexes. The results are shown in Figure 4B. In fact, it is apparent that quenching the emission from the free form actually enhances the total polarization. On the other hand, quenching of the emission from the bound form by using a cationic quencher decreases the steady-state polarization. The cationic cobaltous ion, which itself binds to DNA, efficiently quenches the emission from bound ruthenium cations. The results then are consistent with the presence of both an intercalatively bound species, giving rise to polarization and quenched by cobaltous ion, and a more loosely held surface-bound species, which does not contribute to polarization but is more accessible to ferrocyanide.

Emission Lifetimes. Emission lifetimes of the ruthenium complexes are significantly increased upon binding to DNA.^{8c} These lifetimes have been measured for the enantiomers of the ruthenium complexes with DNAs differing in base sequences, in order to gain further insight into the origin of stereoselectivity. All emission decays measured, except in case of poly[d(GC)] with the Λ enantiomer, are nonexponential. The intercalative binding can significantly reduce the metal complex mobility at the binding site, as shown in polarization experiments, and also can significantly increase the excited-state lifetime. Altered solvent structure and an asymmetric environment can also significantly contribute to these changes. Thus, one would expect a longer lived component for the intercalated metal complex than for the other bound or free forms. A fast exchange among the free and various bound forms can time average these lifetimes. The data obtained for the enantiomers with various DNAs are collected in Table I. The decay profiles are clearly nonexponential and can be fit to a biexponential decay with a short-lived component (~ 550 ns) and a longer lived component ($\sim 2 \mu s$). These lifetimes do not show a clear trend with the base composition of the DNA. However, several features are clear. The lifetime of $Ru(phen)_3^{2+}$ and its optical isomers, under similar conditions in the absence of DNA, was found to be 525 ± 10 ns, and therefore the shorter lived emission may be assigned to the free ruthenium. When ferrocyanide was employed as the quencher, which efficiently quenches the emission from free ruthenium ($k_q = 8.4 \times 10^9 M^{-1} s^{-1}$,^{8d} the two components are still present in the decay profile. Except for intensity differences, the curves are superimposable. This leads us to suggest that the shorter lived emission in fact has significant contributions from the surface-bound form as well. In fact at ruthenium to nucleotide ratios of 1:40 when the binding is essentially complete, this shorter lived component is still a major emitting species. We conclude that the shorter lived species has contributions from the surface-bound form as well as the free form, and the long-lived component is mainly the intercalated complex. Further supporting evidence for this assignment comes from the results of emission lifetime measurements for the Λ isomer with poly[d(GC)] (Table I). The decay profile is, strikingly, a single exponential and has no long-lived component. The polarization values are close to that of the free form (0.0020) and therefore clearly indicate that this enantiomer has little or no intercalation into poly[d(GC)]. Thus, it is very clear that the longer lived component is essentially due to the intercalated metal complex.

Variations in Base Sequence. By use of the methods described above, characteristics of binding of $Ru(phen)_3^{2+}$ to DNAs of various guanine-cytosine (GC) contents were determined. Table I summarizes the parameters obtained for calf thymus DNA, two natural DNAs having particularly low and high GC contents, and two synthetic polymers, poly(dAT) and poly(dGC). Several trends emerge. At first sight it appears that there is no base preference in binding $Ru(phen)_3^{2+}$ to DNA. Values of $K(0)$, obtained by equilibrium dialysis of racemic mixtures, show no particular trend with variations in GC content, except with poly[d(GC)], and are within experimental error. This finding is in contrast to binding studies for the planar metallointercalators $(phen)Pt(en)^{2+}$ and $(terpy)Pt(HET)^+$, both of which displayed a linear dependence of binding affinity on GC content of the DNA.²⁶ The same conclusion may be drawn based upon the Stern-Volmer constants for racemic mixtures in the ferrocyanide quenching experiment.

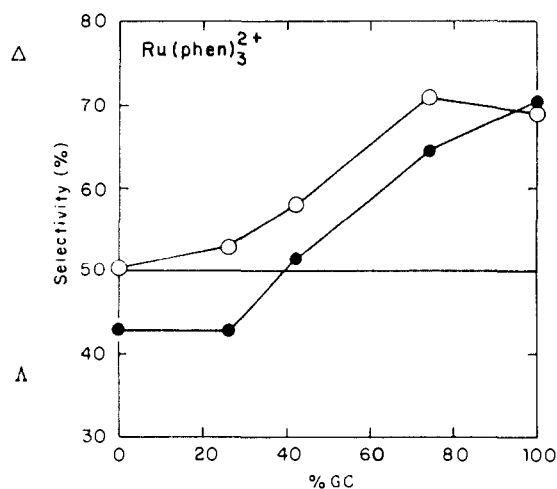


Figure 5. Stereoselectivity, S , associated with binding of $\text{Ru}(\text{phen})_3^{2+}$ to DNAs of varying GC content determined by differences in steady-state polarization (O) and through equilibrium dialysis (●). Polarization results indicate enantioselectivity for intercalation, and the dialysis results, selectivity for total binding.

The quenching results coincide quite closely to that found by equilibrium dialysis, and the Stern–Volmer slopes show no particular variation as a function of percent GC. Emission lifetimes, determined for aerated solutions containing ruthenium and various nucleic acids, also show no clear dependence on GC content (Table I). Each sample showed two components: a short-lived species having a lifetime of ~ 500 ns assigned to surface-bound and free forms, and a longer lived species with a lifetime of ~ 2 μs assigned to intercalated metal complex. The relative intensity of the latter component is highest ($\sim 1:1$) for poly[d(AT)] and becomes lower with increasing GC content. As mentioned earlier, the Δ $\text{Ru}(\text{phen})_3^{2+}$ appears to have almost no intercalated form with poly[d(GC)]. The steady-state polarization for the complexes does reveal a clear dependence on GC content, displaying a maximum at $\sim 50\%$ GC content (Table I). The absolute polarizations for $\text{Ru}(\text{phen})_3^{2+}$ bound to various DNAs, which presumably differ in length and in flexibility, are difficult to compare quantitatively. The polarization measured is maximum for calf thymus DNA, and therefore it is tempting to suggest that intercalation is favored at a 50% GC content or, in other words, in a site containing an equal mixture of the different bases.

In contrast to the ambiguity of information derived from studies of racemic mixtures, a clear trend related to base composition is evident, however, in comparing binding of ruthenium enantiomers to the helix (Table I). At high percent GC values Δ - $\text{Ru}(\text{phen})_3^{2+}$ binds preferentially and shows a smaller quenching constant, K_{SV} , than that seen with the Λ - $\text{Ru}(\text{phen})_3^{2+}$. The opposite is true, however, for DNAs having a low percent GC. Here, the overall selectivity is actually reversed, and Λ - $\text{Ru}(\text{phen})_3^{2+}$ appears to bind preferentially to the helix. Although it is difficult to compare binding parameters, absolute polarization, and quenching rate constants among different DNAs quantitatively, a measurement of relative stereoselectivity by using each of these methods is easily accomplished and significant.

The variation in stereoselectivity with GC content by equilibrium dialysis and by polarization measurements is given in Figure 5. The selectivity, S , is defined here as the amount of Δ - $\text{Ru}(\text{phen})_3^{2+}$ bound per total bound ruthenium. Thus, a value of 0.5 for S corresponds to no chiral discrimination, and $S = 1.0$ represents the enantiospecific association of the Δ - $\text{Ru}(\text{phen})_3^{2+}$ with the polynucleotide. Figure 5 shows the plot of stereoselectivity found in total binding, determined by measuring the optical enrichment in dialysates after equilibrium dialysis of the racemic mixture, and that found in the purely intercalative component as defined by that bound species contributing polarization. Smooth variations with percent GC are seen for both methods, one displaced relative to the other. Thus, an interesting comparison between these two experiments is apparent. By equilibrium dialysis

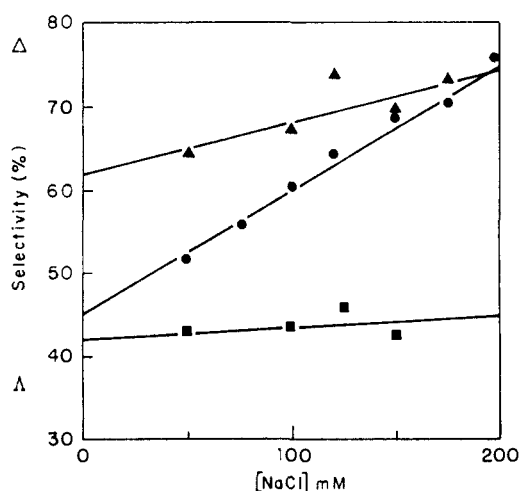


Figure 6. Selectivity in binding $\text{Ru}(\text{phen})_3^{2+}$ isomers to calf thymus DNA (●), 42% GC; *Cl. perfringens* DNA (■), 26% GC; and *M. lysodeikticus* DNA (Δ), 74% GC, as a function of increasing ionic strength of the medium.

the stereoselectivity ranges from 0.73 with high GC content, reflecting a 3:1 preference for the Δ - $\text{Ru}(\text{phen})_3^{2+}$, to a value of 0.43 for poly(dAT), indicating indeed a slight preference (1.33) for Λ - $\text{Ru}(\text{phen})_3^{2+}$. Polarization results, however, show in all cases a preference for Δ - $\text{Ru}(\text{phen})_3^{2+}$, which increases with increasing GC content.

Therefore, the measurement of relative stereoselectivity provides an additional means to characterize specifically the two binding modes of $\text{Ru}(\text{phen})_3^{2+}$ isomers with DNA. Intercalation, the binding mode detected through emission polarization, favors Δ - $\text{Ru}(\text{phen})_3^{2+}$. Furthermore, by polarization, there is a variation in enantiomeric selectivity for intercalation with the guanine–cytosine content of the DNA; while a high level of chiral discrimination is evident with GC-rich DNAs, DNAs rich in adenine–thymines (AT) show essentially no preference for intercalation of $\text{Ru}(\text{phen})_3^{2+}$ isomers. The result suggests a differing local DNA structure, perhaps more compact, as a function of increasing GC content, that may be recognized with binding by the chiral metal complexes. The difference in stereoselectivity between measurements via polarization experiments and through dialysis must reflect the level of discrimination that occurs for the nonintercalative binding mode, the surface-bound component, the component that does not yield significant polarization and is more accessible to quenching by ferrocyanide. This mode of binding then clearly shows a selectivity for Λ - $\text{Ru}(\text{phen})_3^{2+}$ and most likely is independent of GC content. The difference in S between polarization and dialysis is essentially constant, except for poly[d(GC)], with variations in percent GC and has an average S value for the surface-bound component of 0.43. The level of enantiomeric discrimination by this binding mode for Λ - $\text{Ru}(\text{phen})_3^{2+}$ therefore is not high (1.33) but is significant. Finally, given that there is any chiral preference noted, the binding must not be by definition purely a nonspecific electrostatic association. Perhaps this binding mode derives stereoselectively from some association of the metal complex with the asymmetric groove of the DNA helix, where the helix topography may dictate the stereoselectivity.

Variations in stereoselectivity of total binding as a function of ionic strength (50–200 mM Na^+) are given in Figure 6 for the binding of *rac*- $\text{Ru}(\text{phen})_3^{2+}$ to *Cl. perfringens*, calf thymus, and *M. lysodeikticus* DNAs. As the ionic strength is varied over this small range, changes in enantiomeric preferences are evident. The surface-binding component favoring the Λ - $\text{Ru}(\text{phen})_3^{2+}$ persists over this variation in salt, as seen in the slight enantiomeric preference (1.2) of *Cl. perfringens* DNA (74% AT) for Λ - $\text{Ru}(\text{phen})_3^{2+}$. For calf thymus DNA, of intermediate GC content, the fluctuations are most pronounced. As the salt concentration is increased, the preference for Δ - $\text{Ru}(\text{phen})_3^{2+}$ changes from 30% to 300%. In the case of *M. lysodeikticus* DNA, for which the

Table II. Binding of Ruthenium Complexes to Nucleic Acids of Different Structures

complex	nucleic acid	$K(0)$, M^{-1}	quenching slope	S^a
$Ru(phen)_3^{2+}$	calf thymus DNA	6200	440	0.6
	poly(A)·poly(U)	300	na ^b	0.4
	poly(I)·poly(C)	<100	na ^b	
	tRNA	<100	na ^b	
Δ - $Ru(DIP)_3^{2+}$ ^d	T4 (glucosylated) ^c	300	700	0.3
	T4 (glucosylated) calf thymus ^e		350 220	

^a S , as defined above, was determined for total binding by equilibrium dialysis. ^bNot available; binding to RNA does not yield any luminescence enhancements that are susceptible to ferrocyanide quenching. Instead, self-quenching of ruthenium cations along the polymer is found. ^cT4 DNA, 34% GC, is fully glucosylated through hydroxyl methyl substitution at the C5 position of all cytosines, which leads to glucosylation throughout the major groove. ^dFor experiments with Δ - $Ru(DIP)_3^{2+}$, 10% Me₂SO solutions were employed to aid solubility. ^eReference 8c.

chiral discrimination is quite high even at 50 mM sodium ion, increasing the salt leads as well to an increase in stereoselective preference for Δ - $R(phen)_3^{2+}$. It is noteworthy that for all DNAs, with increasing ionic strength, as phosphate-phosphate repulsions along the helix decrease, the enantiomeric selectivity for the Δ - $Ru(phen)_3^{2+}$ increases. This suggests that the stereoselectivity is sensitive to the gradual changes in local DNA structure that are associated with variations in ionic strength.

Binding of Ruthenium Complexes to Other Nucleic Acids. Table II summarizes the low-binding data with polynucleotides obtained for $Ru(phen)_3^{2+}$ and Δ - $Ru(DIP)_3^{2+}$, the bulkier chiral analogue that binds stereospecifically to B DNA. As can be seen in the table, determined by dialysis, $Ru(phen)_3^{2+}$ isomers bind poorly to double-stranded RNAs. Luminescence quenching by ferrocyanide cannot be monitored since no detectable enhancement in luminescence on initial polymer binding is found. Furthermore, no polarization is evident in the ruthenium emission. Hence it appears that intercalative binding of $Ru(phen)_3^{2+}$ to double-stranded RNA does not occur. This contrasts with results obtained for another metallointercalator, (terpy)Pt(HET)⁺.²⁸ Consistent with this result, the level of stereoselectivity determined for poly(A)·poly(U) (the sole RNA polymer for which sufficient binding was found to obtain a measurement of S) is 0.4; only a nonintercalative surface-bound association occurs for $Ru(phen)_3^{2+}$ with RNA, and this binding mode shows a preference for the Δ - $Ru(phen)_3^{2+}$.

Poor binding is evident also for $Ru(phen)_3^{2+}$ and Δ - $Ru(DIP)_3^{2+}$ with T4 DNA glucosylated³³ in the major groove. This result is illustrated in Figure 7 by comparing emission quenching by ferrocyanide of the ruthenium complexes bound to calf thymus with those bound to glucosylated T4. For both species, it is clear that accessibility to the anionic quencher is greater for T4 than for calf thymus; binding to the helix is lower (higher late slopes), given the glucosylation. Interestingly, the quenching curve for Δ - $Ru(DIP)_3^{2+}$ with the T4 DNA is now linear; intercalative tight binding by this complex is precluded. The quenching curve is instead strikingly similar to that seen earlier for Δ - $Ru(DIP)_3^{2+}$ with calf thymus DNA,^{8c} where the Δ - $Ru(phen)_3^{2+}$ could not bind

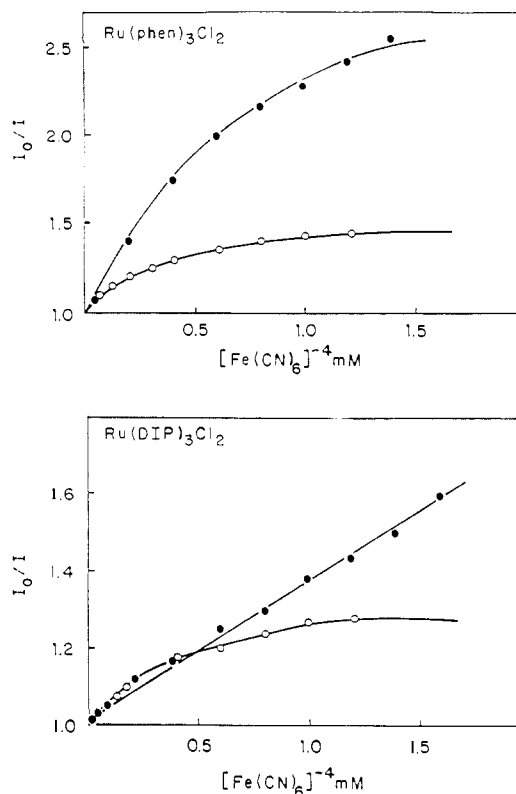


Figure 7. Luminescence quenching with ferrocyanide of $Ru(phen)_3^{2+}$ (top) and Δ - $Ru(DIP)_3^{2+}$ (bottom) bound to calf thymus DNA (O) and glucosylated T4 DNA (●).

the right-handed helix owing to steric constraints. Thus, it appears that Δ - $Ru(DIP)_3^{2+}$ binds to right-handed DNA in the major groove since this binding is shut off upon glucosylation. The same conclusion may be drawn for $Ru(phen)_3^{2+}$. A pronounced increase in accessibility to ferrocyanide quenching is evident, consistent with the decrease in binding. In comparison to Δ - $Ru(DIP)_3^{2+}$, the curve for the phenanthroline complex is not strictly linear however. This slight curvature may reflect the higher probability of $Ru(phen)_3^{2+}$ for finding a four base pair site that is not glucosylated ($P = 0.18$) than for $Ru(DIP)_3^{2+}$, which is much bulkier and may require an eight base pair site ($P = 0.04$). It appears then that $Ru(phen)_3^{2+}$ may also bind to the major groove of the helix. For $Ru(phen)_3^{2+}$ a decrease in binding can be seen as well by equilibrium dialysis; for $Ru(DIP)_3^{2+}$ dialysis cannot be practically performed owing to poor solubility. As shown in Table II, from the value of stereoselectivity, binding of $Ru(phen)_3^{2+}$ to glucosylated T4 most favors Δ - $Ru(phen)_3^{2+}$ ($S = 0.3$). Surface binding along the major groove of the helix is perhaps more favored once the groove is filled with the polar glucose units.

Discussion

The experiments described here support the notion that tris-(phenanthroline)ruthenium(II) cations bind to DNA by two modes: one intercalative and one that is solvent accessible, is surface binding, and most likely involves ligand interactions along the helical groove. The binding affinity of the complex for the helix shows a substantial dependence on ionic strength, consistent with expectations for ionic binding by a divalent cation. The intense metal-to-ligand charge-transfer band of the ruthenium polypyridines provides a useful spectroscopic handle to distinguish binding modes. Kelly et al. have also recently examined the intercalative characteristics of various polypyridylruthenium(II) species.³⁴ The luminescence in the presence of DNA here shows a biexponential decay suggestive of two emitting species. The quenching rates with the ferrocyanide anion also indicate the

(28) Barton, J. K.; Lippard, S. J. *Biochemistry* **1979**, *18*, 2661-2668.

(29) The DNA helix containing an intercalation site that was used for modeling was constructed by inserting the (C₂G)₂ dinucleoside monophosphate fragment with ethidium intercalated³⁰ into the center of the Dickerson dodecamer.³¹ Coordinates for $Ru(phen)_3^{2+}$ isomers were based upon the X-ray determination of the structure of $Ru(DIP)_3^{2+}$.³²

(30) Jain, S. C.; Tsai, C.-C.; Sobell, H. M. *J. Mol. Biol.* **1977**, *114*, 317-331.

(31) Dickerson, R. E.; Drew, H. R.; Conner, B. N.; Wing, R. M.; Fratini, A. V.; Kopka, M. L. *Science (Washington, D.C.)* **1982**, *216*, 475.

(32) Goldstein, B. M.; Barton, J. K.; Berman, H. M., submitted for publication.

(33) The T-even phage DNAs show with glucosylation a B-like structure but with the major groove of the helix filled with glucose units. See: Mokol'skii, M. A.; Kaiparova, K. A.; Mokol'skaya, T. D. *Mol. Biol. (Moscow)* **1972**, *6*, 714-731.

(34) Kelly, J. M.; Tossi, A. B.; McConnell, D. J.; Ohvign, C. *Nucleic Acids Res.* **1985**, *13*, 6017-6034.

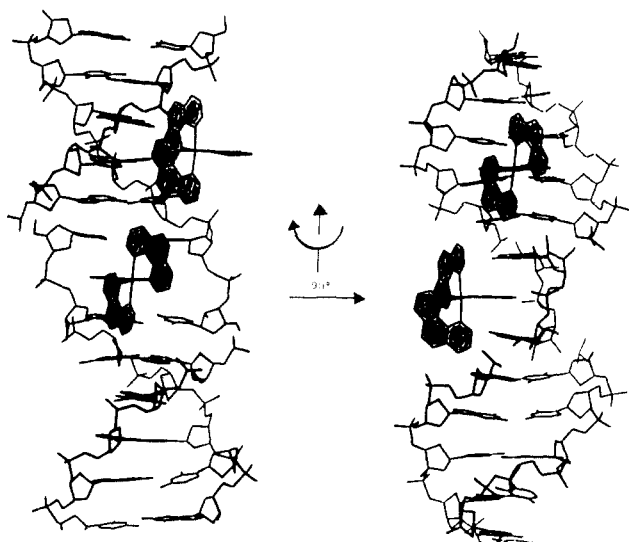


Figure 8. Two binding modes of $\text{Ru}(\text{phen})_3^{2+}$ isomers to the helix. Left: The Δ isomer (bottom) is shown intercalated into the helix. The preference for intercalation by $\Delta\text{-Ru}(\text{phen})_3^{2+}$ is shown in this view since the disposition of the nonintercalated ligands follows the right-handed groove. The Λ isomer (top) is shown bound electrostatically along the groove, with the ligands lining the helical surface. Right: The same model after 90° rotation about the helical axis. Intercalation of the Δ isomer is shown below, with one ligand stacked between base pairs. The basis for enantioselectivity of surface binding is seen for the Λ isomer (above) since here the disposition of its ligands follows the right-handed groove.

presence of more than one bound species since curvature is observed in the Stern–Volmer plot. The two species display a differential accessibility to the aqueous phase quencher. Steady-state polarization experiments further support the presence of two bound species, one of which is the intercalative component that preserves polarization on the time scale of the emission. The polarization is enhanced by quenching with ferrocyanide but is reduced upon quenching with cobaltous ion, which quenches the bound species.

Measurements of stereoselectivity of binding provide a sensitive means to describe the binding modes with some structural detail. Enantiomeric selectivity is associated with each mode of binding to right-handed DNAs: intercalation favoring $\Delta\text{-Ru}(\text{phen})_3^{2+}$ and the electrostatic groove association, which we call surface binding, weakly favoring $\Lambda\text{-Ru}(\text{phen})_3^{2+}$. Figure 8 shows our structural model for the interaction of $\text{Ru}(\text{phen})_3^{2+}$ isomers with B DNA. The chiral metal complexes are shown bound along the major groove of the helix, consistent with the greatly decreased binding of the complexes to T4 DNA, which is extensively glucosylated in the major groove. The $\Delta\text{-Ru}(\text{phen})_3^{2+}$ cation is intercalated within the helix,²⁹ with one ligand partially inserted and stacked between the base pairs. The surface binding for $\Lambda\text{-Ru}(\text{phen})_3^{2+}$ in the major groove is also shown. The model on the left of Figure 8 depicts the structure viewed into the major groove. In this view the nonintercalated ligands of the $\Delta\text{-Ru}(\text{phen})_3^{2+}$ have a disposition that matches the direction of the right-handed helix. The basis for the chiral discrimination associated with intercalation, that is the different steric interactions of nonintercalated ligands with the asymmetric DNA helix, is evident in this view. On the basis of its symmetry relative to the right-handed helix, it is apparent that $\Delta\text{-Ru}(\text{phen})_3^{2+}$ would intercalate preferentially to B DNA due to favorable steric interactions. In contrast, the $\Lambda\text{-Ru}(\text{phen})_3^{2+}$ cation, shown above $\Delta\text{-Ru}(\text{phen})_3^{2+}$, is bound against the groove of the helix. Two ligands of $\Lambda\text{-Ru}(\text{phen})_3^{2+}$ are seen to surround the helical column, the phenanthroline perpendicular and juxtaposing the base pairs. Perhaps hydrophobic interactions of ligands along the groove lend stability that supplement electrostatic stabilization. Certainly this binding would result in greater accessibility to ferrocyanide than intercalation. In addition, the retention of steady-state polarization from the loose nonspecific association along the groove is unlikely. The model to the right shows the same complexes viewed after a 90° rotation about the

helical axis. Intercalative stacking of $\Delta\text{-Ru}(\text{phen})_3^{2+}$ is clearly visible. But importantly the basis for the enantiomeric discrimination associated with the groove binding becomes clear in this view. Note it is the asymmetry of the two groove-bound ligands of $\Delta\text{-Ru}(\text{phen})_3^{2+}$ that matches the asymmetric right-handed helical column. The third ligand is projected outward, toward the viewer. It is therefore interesting to notice that it is surface groove binding that requires a complementary asymmetry in structures, $\Lambda\text{-Ru}(\text{phen})_3^{2+}$ bound against a right-handed helix, whereas intercalation, inserting into the base-paired structure, is best when symmetries are matched; as a result $\Delta\text{-Ru}(\text{phen})_3^{2+}$ intercalates selectively into a right-handed helix. This stereochemical criterion was noted also with respect to the complementary coordination of bis(phenanthroline)ruthenium(II) species onto a B DNA helix.⁹

Because stereoselectivity is associated with the binding to the helix, sequence-dependent variations in the structures of the bound complexes may be examined. On the basis of two different methods of analysis, no variations in overall binding constant are found, within experimental error, as a function of the guanine–cytosine content of the DNA. Nonetheless, by using measurements of optical enrichment or differential binding effects between enantiomers, apparently more sensitive or subtle indicators, variations in binding with base composition become apparent. The steady-state polarization results show that sequence-dependent variations are associated with intercalation. With increasing GC content, the enantiomeric preference for DNA binding of $\Delta\text{-Ru}(\text{phen})_3^{2+}$ increases appreciably.

Based on the intercalative model, then, some suggestion as to a sequence-dependent variation in local DNA structure may be made. The enantiomeric selectivity for intercalation depends on the size of the helical groove relative to the diameter (sterically excluded distance) of the chiral metal complex. If the DNA groove is wider than the complex, there is no enantiomeric discrimination; if the complex is much larger than the groove, as for $\text{Ru}(\text{DIP})_3^{2+}$, the binding is stereospecific. Hence the degree of stereoselectivity becomes in a sense a “molecular yardstick” in solution for helical groove size. The $\text{Ru}(\text{phen})_3^{2+}$ cation must have a diameter (16 Å) close to the groove size of the DNA helix, and therefore small variations in groove size are sensitively expressed in changes in the degree of stereoselective binding by the ruthenium cations. Note that the measurement extends beyond the site of intercalation for approximately two base pairs above and two base pairs below for $\text{Ru}(\text{phen})_3^{2+}$. In terms of this model, then, it may be suggested that GC-rich sequences stack more closely to one another, yielding a smaller, tighter groove than AT-rich sequences. This would explain the increase in the degree of stereoselectivity associated with intercalation for DNAs of higher GC. This idea is consistent also with thermodynamic measurements and calculations of base pair stacking energies.^{35,36} Compressions along the helix axis direction can be detected as well through variations in the ionic strength of the medium. With increasing concentration of sodium ion, phosphate–phosphate repulsions are neutralized and the helix contracts. Consistent with this notion, as the sodium concentration is increased, the stereoselective preference for $\Delta\text{-Ru}(\text{phen})_3^{2+}$ also increases. The variation in discrimination is seen to be the largest for calf thymus DNA, of intermediate GC content and therefore with a groove very close in size to the phenanthroline complex, whereas only small variations are noted for both *Cl. perfringens* DNA containing a wider groove and *M. lysodeikticus* with a smaller groove and thus already binding enantiomers with high selectivity. It is interesting to note that the major effect of salt, based on the dialysis results, appears to be on stereoselective intercalation rather than on the level of groove binding. Thus, the binding results and

(35) (a) Gotoh, O.; Tagashira, Y. *Biopolymers* **1981**, *20*, 1033–1042. (b) Borer, B. N.; Dengler, B.; Tinoco, I., Jr.; Uhlenbeck, O. C. *J. Mol. Biol.* **1974**, *86*, 843–853. (c) Ornstein, R. L.; Rein, R.; Breen, D. L.; MacElroy, R. D. *Biopolymers* **1978**, *17*, 2341–2360.

(36) Comparisons of sequence variations in groove widths cannot be made with crystal structure results, however, since the B DNA dodecamer does not contain a sufficient variety of the sequence arrangements.

measures of enantiomeric selectivity for these small chiral metal complexes provide a unique probe for local DNA structure in solution. *The size and shape of the metal complex may be tuned to the DNA helical groove size.*

It is interesting, finally, to compare binding parameters of the complexes with nucleic acids differing markedly in structure. Binding to double-stranded RNA is extremely poor as is binding to a DNA with the major groove filled by glucosylation. Binding, therefore, must be preferred through the major groove. This observation is understandable structurally; the minor groove of B DNA is apparently too small to accommodate either isomer. For double-stranded RNA, which has an A-like conformation, what was the B-form major groove is now smaller and deeper while the minor groove is more shallow and extended.³⁷ Perhaps based upon electronic considerations, intercalation of the phenanthroline ligand is favored from the major groove. Since this groove is narrowed for a RNA helix, binding to the RNA helix is not high. It is interesting to notice that, for both these polymers, glucosylated T4 and double-stranded RNAs, some nonintercalative surface binding is still apparent. Indeed the enantiomeric preference for Δ -Ru(phen)₃²⁺ may be somewhat enhanced. An explanation may be in the fact that both of these polynucleotides contain shallow surfaces along the helical groove. Perhaps the polar glucose units

filling the major groove or the shallow base pair surface of the RNA minor groove facilitate binding of the Δ -Ru(phen)₃²⁺ cations by the surface-bound mode, optimizing hydrophobic interactions between the phenanthroline ligands and shallow helical surfaces. This binding interaction could potentially provide the basis for probes of the A conformation.

In summary, the interaction of the chiral metal complexes with polynucleotides may be described in detail by taking advantage of the spectroscopic properties of the ruthenium center combined with measurements of enantiomeric preferences. Two binding modes, one based upon intercalation and one upon surface binding, have been characterized, and both display chiral discrimination. Given these binding models, photophysical experiments coupled with measurements of enantiomeric selectivity may be used to examine subtle features of the polynucleotide structure. Small molecules and chiral complexes in particular offer unique structural probes in solution for the local conformation of sites along the polymer.

Acknowledgment. We thank the National Institute of General Medical Sciences, the National Science Foundation, and the Army Office of Research for their generous support of this work. We thank also Dr. Charles Doubleday for providing the software employed in our single photon counting analyses.

(37) Arnott, S.; Hukins, D. W. L.; Dover, S. D.; Fuller, W.; Hodgson, A. R. *J. Mol. Biol.* **1973**, *81*, 107–122.

Registry No. Δ -Ru(phen)₃²⁺, 19368-51-5; Λ -Ru(phen)₃²⁺, 24162-09-2; guanine, 73-40-5; cytosine, 71-30-7.

Communications to the Editor

Paramagnetic Cobalt(III) Complexes of Polyanionic Chelating Ligands

Terrence J. Collins,*¹ Thomas G. Richmond,²
Bernard D. Santarsiero, and Brian G. R. T. Treco

Contribution No. 7288, The Chemical Laboratories
California Institute of Technology
Pasadena, California 91125

Received September 16, 1985

Our approach to the problem of finding new oxidizing agents³ is to investigate the coordination chemistry of novel polyanionic chelating (PAC) ligands (e.g., **1**, **2**).^{4–7} Ligand **1** forms stable

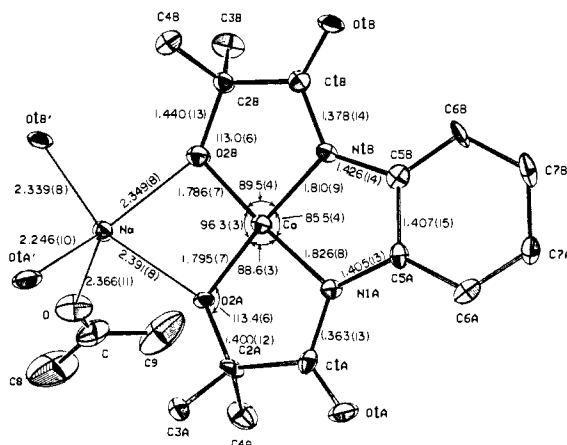
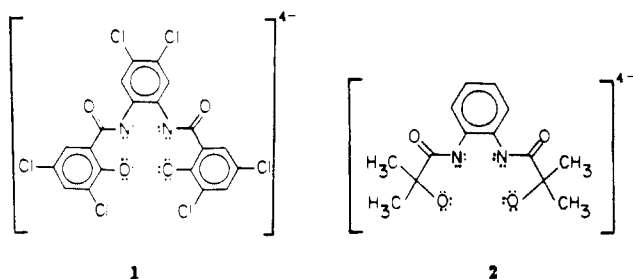


Figure 1. Molecular structure of Na[(η^4 -**2**)]-acetone.

octahedral cobalt(III) and cobalt(IV) complexes,⁷ but here we show that **2**, which has a greater donor ability, stabilizes Co(III) in the rare square-planar geometry. Well-resolved, paramagnetically shifted, solution ¹H NMR spectra have been measured for these intermediate and high-spin cobalt(III) complexes.⁸

Reaction of Co(O₂CCH₃)₂ with 1 equiv of H₄-**2** and excess NaOH in ethanol under air gives a deep green solution containing [Co(η^4 -**2**)]⁻, which can be isolated (ca. 70%) as the Na⁺ salt **3**

(1) Dreyfus Teacher-Scholar 1986–1990.
(2) Myron A. Bantrell Research Fellow, California Institute of Technology, 1983–1985. Present address: Department of Chemistry, University of Utah, Salt Lake City, UT 84112.
(3) "Report of the International Workshop on Activation of Dioxygen Species and Homogeneous Catalytic Oxidations", Galzignano, Padua, Italy, June 28–29, 1984; Collins, T. J., Ed.; University of Padua: Padua, 1984.
(4) Anson, F. C.; Christie, J. A.; Collins, T. J.; Coots, R. J.; Furutani, T. T.; Gipson, S. L.; Keech, J. T.; Krafft, T. E.; Santarsiero, B. D.; Spies, G. H. *J. Am. Chem. Soc.* **1984**, *106*, 4460–4472.

(5) Chrstie, J. A.; Collins, T. J.; Kraft, T. E.; Santarsiero, B. D.; Spies, G. H. *J. Chem. Soc., Chem. Commun.* **1984**, 198–199.
(6) Collins, T. J.; Santarsiero, B. D.; Spies, G. H. *J. Chem. Soc., Chem. Commun.* **1983**, 681–682.
(7) Anson, F. C.; Collins, T. J.; Coots, R. J.; Gipson, S. L.; Richmond, T. G. *J. Am. Chem. Soc.* **1984**, *106*, 5037–5038.
(8) van der Put, P. J.; Schilperoord, A. A. *Inorg. Chem.* **1974**, *13*, 2476–2481.